



ALMA MATER STUDIORUM  
UNIVERSITÀ DI BOLOGNA

ARCHIVIO ISTITUZIONALE  
DELLA RICERCA

## Alma Mater Studiorum Università di Bologna Archivio istituzionale della ricerca

Hexabromocyclododecanes Are Dehalogenated by CYP168A1 from *Pseudomonas aeruginosa* Strain HS9

This is the final peer-reviewed author's accepted manuscript (postprint) of the following publication:

*Published Version:*

Huang L., Wang W., Zanaroli G., Xu P., Tang H. (2021). Hexabromocyclododecanes Are Dehalogenated by CYP168A1 from *Pseudomonas aeruginosa* Strain HS9. *APPLIED AND ENVIRONMENTAL MICROBIOLOGY*, 87(17), 1-11 [10.1128/AEM.00826-21].

*Availability:*

This version is available at: <https://hdl.handle.net/11585/858833> since: 2022-02-15

*Published:*

DOI: <http://doi.org/10.1128/AEM.00826-21>

*Terms of use:*

Some rights reserved. The terms and conditions for the reuse of this version of the manuscript are specified in the publishing policy. For all terms of use and more information see the publisher's website.

This item was downloaded from IRIS Università di Bologna (<https://cris.unibo.it/>).  
When citing, please refer to the published version.

(Article begins on next page)

1 **Hexabromocyclododecanes are dehalogenated by CYP168A1 from a**  
2 ***Pseudomonas* strain HS9**

3

4 Ling Huang<sup>1†</sup>, Weiwei Wang<sup>1†</sup>, Giulio Zanaroli<sup>2</sup>, Ping Xu<sup>1</sup> and Hongzhi Tang<sup>1\*</sup>

5

6 <sup>1</sup>State Key Laboratory of Microbial Metabolism, and School of Life Sciences &  
7 Biotechnology, Shanghai Jiao Tong University, Shanghai 200240, People's Republic  
8 of China

9 <sup>2</sup>Department of Civil, Chemical, Environmental and Materials Engineering (DICAM),  
10 University of Bologna, Bologna 40131, Italy

11

12 †These authors contributed equally to this study.

13 \*Corresponding author: H. Z. Tang; Mailing address: School of Life Sciences &  
14 Biotechnology, Shanghai Jiao Tong University, Shanghai 200240, P. R. China;

15 E-mail: [tanghongzhi@sjtu.edu.cn](mailto:tanghongzhi@sjtu.edu.cn); Tel: +86-21-34204066; Fax: +86-21-34206723.

16 **Abstract**

17 Hexabromocyclododecanes (HBCDs) are widely used brominated flame retardants,  
18 which cause antidiuretic hormone syndrome and even induce cancer. However, little  
19 information is available about the degrading mechanisms of HBCDs. In this study,  
20 genomic, proteomic analyses, RT-qPCR and gene knockout assays reveal that a  
21 cytochrome P450 encoding gene is responsible for the HBCD catabolism in  
22 *Pseudomonas aeruginosa* HS9. CO-difference spectrum of the enzyme CYP168A1  
23 was matched to P450 character and proved by western blot analysis and UV-visible.  
24 We demonstrate that the reactions of debromination and hydrogenation are carried out  
25 one after another based on detection of the metabolites pentabromocyclododecanols  
26 (PBCDOHs), tetrabromocyclododecadiols (TBCDDOHs) and Br<sup>-</sup> ion. In the <sup>18</sup>O  
27 isotope experiments, PBCD<sup>18</sup>OHs were only detected in the H<sub>2</sub><sup>18</sup>O group, proving that  
28 the added oxygen is derived from H<sub>2</sub>O not from O<sub>2</sub>. This study elucidates the  
29 degrading mechanism of HBCDs by *Pseudomonas*.

30 **Importance**

31 Hexabromocyclododecanes (HBCDs) are environmental pollutants, which are widely  
32 used in industry. In this study, we identified and characterized a novel key  
33 dehalogenase CYP168A1 responsible for the HBCDs degradation from a  
34 *Pseudomonas aeruginosa* strain HS9. This study provides new insights into  
35 understanding biodegradation of HBCDs.

## 36 **Introduction**

37 Hexabromocyclododecanes (HBCDs) are the second most widely used brominated  
38 flame retardants (BFRs), and are utilized in building materials, electronics, textiles,  
39 and plastics (1). They are a threat to human health due to causing antidiuretic  
40 hormone syndrome and even inducing cancer. Microorganisms play important roles in  
41 degradation and detoxification of pollutants of HBCDs (2). However, little  
42 information is available about molecular and biochemical mechanisms, particularly  
43 how functional proteins relate to debromination. Only two dehalogenases, LinA and  
44 LinB from the hexachlorocyclohexane transformation strain *Sphingobium indicum*  
45 B90A, can convert HBCD to different debrominated products. LinA selectively  
46 catalyzes the transformation of  $\beta$ -HBCDs to  
47 *1E,5S,6S,9R,10S*-pentabromocyclododecene (PBCDE), while LinB transforms all  $\alpha$ -,  
48  $\beta$ -, and  $\gamma$ -HBCD isomers to pentabromocyclododecanols (PBCDOHs) and even  
49 tetrabromocyclododecadiols (TBCDDOHs) (3-4). The kinetics and stereochemistry of  
50 LinB-catalyzed  $\gamma$ -HBCD transformation have been described in detail, with  $K_m$ ,  $k_{cat}$ ,  
51 and  $k_{cat}/K_m$  values at  $1.82 \pm 0.60 \mu\text{mol/L}$ ,  $0.25 \pm 0.10 \mu\text{mol/L/h}$  and  $13.0 \pm 6.2$   
52  $\text{L/mol/s}$ . The results suggest that LinB has a high capability to dehalogenate  $\gamma$ -HBCD  
53 (5).

54 Catalytic enzyme resources from bacteria are abundant, and cytochrome P450  
55 enzymes (CYPs) are the key enzymes responsible for the degradation of numerous  
56 endogenous compounds. CYPs are involved in the degradation and detoxification of  
57 multiple toxicants, such as herbicides, xenobiotic poly aromatic hydrocarbons,

58 halogenated aromatics, and polychlorinated biphenyls (6-10). Hydroxylation is the  
59 typical metabolic reaction of xenobiotics catalyzed by CYPs. Transformed CYP81As  
60 from *Echinochloa phyllopogon* decreased—the susceptibility of *Arabidopsis* to  
61 clomazone (11-12). Mammalian CYPs (CYP1 family) degrade dibenzo-*p*-dioxins  
62 (PCDDs) with efficient activity, and the rat CYP1A1 family also showed high activity  
63 towards 2,3,7-trichloro-dibenzo-*p*-dioxin, with the detection of hydroxylated products,  
64 8-hydroxy-2,3,7-trichloro-dibenzo-*p*-dioxins (13). CYP101 dehalogenates  
65 hexachlorobenzene with a different metabolic method, in which the halogen atoms are  
66 replaced by hydroxyl groups (14). CYP2E1 from *Nicotiana tabacum*, CYP3A4 from  
67 human liver and CYPs (CYP71C3v2, CYP71C1, CYP81A1 and CYP97A16) from  
68 maize can metabolize HBCDs, and the hydroxylated metabolites OH-HBCDs,  
69 OH-PBCDs and OH-TBCDs have been detected (15-20). However, the substitution  
70 reaction of HBCDs by CYPs is rarely reported.

71 Previous work by our research group on *Pseudomonas aeruginosa* HS9 indicated  
72 that HBCDs could be degraded to PBCDOHs. Strain HS9 was reported to be a  
73 HBCD-metabolizing bacterium based on its ability to convert HBCDs to PBCDOHs  
74 or tetrabromocyclododecene (TBCDe), dibromocyclododecadiene (DBCDi), and  
75 cyclododecatriene (CDT) (21). In this study, the whole-genome sequence of strain  
76 HS9 was sequenced and analyzed, and putative genes for HBCD degradation were  
77 elucidated. By combining metabolite analysis with real-time fluorescence  
78 quantification experiments (RT-qPCR), the cytochrome P450 enzyme CYP168A1 was  
79 considered as the initial dehalogenase in HBCD metabolism. The gene *cyp168A1* was

80 cloned and expressed in *Escherichia coli*. The subsequent enzymatic properties were  
81 investigated on the purified CYP168A1.

82

### 83 **Materials and methods**

84 **Chemicals.** 1, 2, 5, 6, 9, 10-Hexabromocyclododecanes (HBCDs,  $\geq 95\%$ ) were  
85 purchased from Anpel (New Jersey, USA). Hexachlorobenzene (HCB,  $\geq 95\%$ ) was  
86 purchased from AccuStandard (Connecticut, USA). Ethyl acetate, methanol, and all  
87 the other reagents and solvents used in this study were of analytical grade.

88

89 **Strains and culture media.** *Pseudomonas aeruginosa* HS9 was isolated by our  
90 research group in previous work, and it can be obtained from the China Center for  
91 Type Culture Collection (CCTCC) under accession M 2019094 (20). *Escherichia coli*  
92 DH5 $\alpha$  and BL21(DE3) (Novagen, Inc. USA) were used for plasmid construction and  
93 protein expression, respectively. Lysogeny broth (LB), containing 5 g/L yeast  
94 extraction, 10 g/L tryptone and 5 g/L NaCl, or LB agar (1.5% wt/vol) plates with  
95 appropriate antibiotics were used to culture *E. coli* (22). *E. coli* harboring each of the  
96 constructed plasmids was grown at 37°C, 200 rpm with 50 mg/L kanamycin or 100  
97 mg/L ampicillin for pET28a or pETduet-1 vectors. Strain HS9 was grown at 30°C in  
98 mineral salt medium (MSM) containing 5.0 g/L K<sub>2</sub>HPO<sub>4</sub>, 3.7 g/L KH<sub>2</sub>PO<sub>4</sub>, 1.0 g/L  
99 Na<sub>2</sub>SO<sub>4</sub>, 0.2 g/L MgSO<sub>4</sub>·7H<sub>2</sub>O, 2.0 g/L NH<sub>4</sub>Cl and 0.5 mL 2,000-times trace elements  
100 solution. The trace elements solution consisted of 0.3 g/L FeCl<sub>2</sub>·4H<sub>2</sub>O, 0.038 g/L  
101 CaCl<sub>2</sub>·6H<sub>2</sub>O, 0.02 g/L MnCl<sub>2</sub>·4H<sub>2</sub>O, 0.014 g/L ZnCl<sub>2</sub>, 0.0124 g/L H<sub>3</sub>BO<sub>3</sub>, 0.04 g/L

102  $\text{Na}_2\text{MoO}_4 \cdot 2\text{H}_2\text{O}$  and 0.0034 g/L  $\text{CuCl}_2 \cdot 2\text{H}_2\text{O}$  (21).

103

104 **Genome sequencing and proteomic assay of strain HS9.** The genomic DNA of  
105 strain HS9 was extracted using a Wizard genomic purification kit A1125 (Promega,  
106 USA). Genome sequencing was performed on the Illumina Hiseq-2000 platform.  
107 Functional genes were predicted and annotated with the Rapid Annotations using  
108 Subsystems Technology (RAST) annotation server (23). This whole genome sequence  
109 project was submitted to GenBank under accession GCA\_003319235.1. Proteomic  
110 analysis comparing the protein expression of cells incubated in the presence or  
111 absence of 1 mg/L HBCDs MSM media was carried out as follows. Strain HS9 was  
112 cultured in 2 L flasks containing 1 L HBCDs-MSM. As a control group, strain HS9  
113 was grown in sodium citrate medium. A total of 10 L of culture were collected during  
114 the exponential phase. Both groups were detected with three biological replicates (22).

115

116 **Quantitative RT-qPCR.** Total RNA was isolated from strain HS9 incubated in the  
117 presence or absence of 1 mg/L HBCD MSM media, using a total RNA kit (Tiangen,  
118 China). Total cDNA was synthesized using a SuperScript III reverse transcriptase  
119 (Invitrogen, USA). The 20  $\mu\text{L}$  reverse transcription reaction system contained 1.0  $\mu\text{g}$   
120 total RNA, 0.5 mM dNTP mix, 200 U transcriptase, and 12.5 ng random primers. The  
121 reactions were performed according to the manufacturer's protocols. RT-qPCR was  
122 then carried out using the CEX96 real-time PCR detection system (Bio-Rad) with a  
123 SYBR green I Real Master Mix (TianGen, China). All the data of candidate genes was



124 normalized to the expression level of 16S rRNA and presented as relative to the  
125 expression level in cells growing in the absence of HBCDs. All detections were  
126 performed with three replicates (23–25).

127

128 **Expression and purification of heterologous expressed His-CYP168A1.** The DNA  
129 fragment of *cyp168A1* was amplified by pfu DNA polymerase (New England Biolabs,  
130 Ipswich, MA) with primers Fcyp168A1  
131 (CCGGAATTCCTACTCGCAGGTCTTCTGAG) and Rcyp168A1  
132 (CCCAAGCTTATGGACGACGCATTCAGCGA), in which the enzyme digestion  
133 sites (*Eco*RI and *Hind*III) are underlined. The double enzyme digested DNA  
134 fragments were ligated into expression vector pET28a, which incorporates 6 ×  
135 Histidine tags. Then, the constructed plasmid pET28a-*cyp168A1* was transferred into  
136 *E. coli* (BL21) for heterologous expression. The culture was induced by adding 0.6  
137 mM isopropyl β-D-thiogalactopyranoside (IPTG) after the optical density at 600 nm  
138 (OD<sub>600</sub>) reached 0.6 to 0.8. Then, the culture was incubated at 30°C for 10 h. *E. coli*  
139 was harvested by centrifuging at 4,000 rpm for 20 min, and the pellet was  
140 re-suspended with nickel column balance buffer (20 mM NaH<sub>2</sub>PO<sub>4</sub>-Na<sub>2</sub>HPO<sub>4</sub>, 300  
141 mM NaCl, 10 mM imidazole, 6 M urea, pH 8.0); urea was used to denature the  
142 proteins to enhance solubility (26). The cell suspension was broken by repetitive  
143 sonication at 4°C, and the cell debris was removed by centrifugation at 10,000 rpm for  
144 40 min. The his-CYP168A1 was loaded into the nickel column, and then washed by  
145 gradient imidazole buffers from 10, 40, 70, 100 to 300 mM (27). The residual

146 imidazole in the eluted buffer was removed by gradient dialysis from buffer I (20 mM  
147  $\text{KH}_2\text{PO}_4\text{-K}_2\text{HPO}_4$ , 4 M urea, 5% glycerol, 1% glycine, 1‰ mercaptoethanol, pH 8.0)  
148 for 2 h, to buffer II (20 mM  $\text{KH}_2\text{PO}_4\text{-K}_2\text{HPO}_4$ , 2 M urea, 5% glycerol, 1% glycine,  
149 1‰ mercaptoethanol, pH 8.0) for 2 h, and then to buffer III (20 mM  $\text{KH}_2\text{PO}_4\text{-K}_2\text{HPO}_4$ ,  
150 5% glycerol, 1% glycine, 1‰ mercaptoethanol, pH 8.0) for 3 h. CYP168A1 was  
151 successively refolded *in situ* through a gradient of decreased urea concentrations (26).

152

153 **Western blot analysis and UV-vis characterization of purified CYP168A1.** The  
154 purified CYP168A1 was determined by western blot analysis, using an anti-6 × His  
155 tag® antibody (Abcam, China). The purified CYP168A1 was diluted 10, 100, and  
156 1,000 times, and 10 μL was transferred to PVDF film, respectively. The carbon  
157 monoxide (CO)-difference spectrum was performed in buffer (50 mM  
158  $\text{KH}_2\text{PO}_4\text{-K}_2\text{HPO}_4$ , 1‰ mercaptoethanol, 5% glycerol, pH 8.0) at 20°C, respectively,  
159 in a 0.5-mL quartz cuvette with a 1-mm path length. Protein CYP168A1 was reduced  
160 by adding 10 mM dithionite, and the CO complex was performed by slow bubbling  
161 with CO gas for 1 min 30 s (27).

162

163 **Construction of electron-supplying system and enzyme activity.** To test the *in vitro*  
164 activity of CYP168A1, sufficient electrons must be supplied to the reaction system.  
165 Therefore, an electron-supplying system (named as FdFNR) was constructed by  
166 combining a 4Fe-4S ferredoxin (HS1040) (Fd) and a NAD(P)H-dependent ferredoxin  
167 reductase (HS6332) (FNR) with a glycine linker (GGGGG). The combined DNA

168 fragment was ligated to expression vector pETduet-1 at the second multiple cloning  
169 site (MCS). The protein was induced by adding 0.2 mM IPTG after the OD<sub>600</sub> reached  
170 0.6 to 0.8; then, the culture was incubated at 16°C for 10 h. Ultimately, the cells were  
171 broken in PBS buffer with the same method in the paragraph of CYP168A1  
172 purification, and it was used as the electron-supplying cell free system. The electron  
173 supplying ability was determined with potassium ferricyanide (K<sub>3</sub>[Fe(CN)<sub>6</sub>]) as the  
174 receptor of the free donor, and NADPH as the source of donor. Absorbance of  
175 K<sub>3</sub>[Fe(CN)<sub>6</sub>] at 340 nm was measured and the color feature (yellow) of K<sub>3</sub>[Fe(CN)<sub>6</sub>]  
176 was captured. To test the enzyme activity of CYP168A1 with HBCDs, 1 mg/L  
177 HBCDs, 0.4 mM NADH, 5 µg purified CYP168A1 and 1 mL cell-free system were  
178 mixed, and the reaction system was incubated under different reaction conditions. The  
179 decrease in HBCD concentration was used to calculate enzyme activity. To test the  
180 effect of metal ions on enzyme activity, 10 mM chloride salts (NiCl<sub>2</sub>, CoCl<sub>2</sub>, CaCl<sub>2</sub>,  
181 CuCl<sub>2</sub>, MnCl<sub>2</sub>, ZnCl<sub>2</sub>, MgCl<sub>2</sub>, KCl, FeCl<sub>2</sub> and NaMoO<sub>4</sub>) were separately added to  
182 reaction system.

183

184 **<sup>18</sup>O isotope experiments and analysis.** To confirm the source of the oxygen atom  
185 incorporated into the HBCD degradation products, <sup>18</sup>O<sub>2</sub> and H<sub>2</sub><sup>18</sup>O were used to  
186 supply oxygen atoms for CYP168A1 reactions. The <sup>18</sup>O<sub>2</sub> labeling reaction and  
187 anaerobic assay were performed in an anaerobic workstation AW200SG (Electrotek  
188 Ltd, UK). After excluding air for 1 h by N<sub>2</sub> atmosphere, all the liquid (1 mL FdFNR  
189 buffer, 5 µg purified CYP168A1) was exposed to an N<sub>2</sub> atmosphere for 30 min to

190 remove O<sub>2</sub>. An activity assay system (equal to the system for enzyme activity  
191 detection) that was cell free containing enzyme and NADH was dried and dissolved in  
192 H<sub>2</sub><sup>18</sup>O. All reactions were carried out at 30°C for 6 h. After terminating the reaction by  
193 adding 10 μL HCl (11.64 M) to the 1 mL reaction system, HBCDs were extracted by  
194 using an equal volume of ethyl acetate. Then, samples were mixed using vortex  
195 oscillation for 30 s. Before detection, the upper organic phase was concentrated 30  
196 times. Samples were analyzed using ultra-high-performance liquid  
197 chromatography/time-of-flight mass spectrometry (UPLC-TOF/MS).

198 HBCDs or its products in activity assay experiments and the <sup>18</sup>O isotope  
199 experiments were quantified by UPLC-TOF/MS, equipped with an Eclipse XDB C18  
200 analytical column (5 μm, 4.6 × 150 μm, Keystone Scientific, Agilent). HBCDs in  
201 samples used for products detection were extracted as the above described, and then,  
202 the organic phase was concentrated about 1,000 times. A mobile phase of water and  
203 methanol at a flow rate of 0.25 mL/min was applied for the target compounds. The  
204 proportional gradient of the mobile phase was started at 95% methanol, and increased  
205 linearly to 100% over 25 min, then decreased directly to 95% for 10 min. For mass  
206 spectrometric analysis, the ionization source was run in negative mode, and MS  
207 detection was set from 0 to 1,700 *m/z*. All target compounds were extracted based on  
208 their hydrogen adduct ions [M+H]<sup>-</sup> at *m/z* and characterization of bromine isotope  
209 (28).

210

211 **Bromide detection.** The detection of bromide was conducted on an ion

212 chromatograph coupled with an AS11-HC negative ion column (ICS-5000+, Thermo  
213 Fisher, Germany). The samples were prepared by terminating the reaction by adding  
214 10  $\mu$ L HCl to the 1 mL reaction system, followed by centrifugation-at 12,000 rpm for  
215 5 min to remove the proteins.

216

217 **Gene deletion and complementation.** The suicide vector pK18*mobsacB-Gm* used  
218 for gene deletion was derived from pK18*mobsacB* by replacing the kanamycin  
219 resistance gene with a gentamicin resistance gene (from plasmid pUCTn7T).  
220 Upstream (600 bp) and downstream (600 bp) fragments close to the target gene were  
221 amplified and aligned using fusion PCR, the primers and corresponding PCR  
222 functions used in this study were listed in Table 1. The constructed plasmid  
223 pK18*mobsacB-Gm-cyp168A1AB* was transferred from the *E. coli* donor strain S17-1  
224 to *P. aeruginosa* HS9 by conjugal transfer. Donor strain S17-1 and recipient strain  
225 HS9 were mixed with a volume rate at 5:1 - 10:1 and cultured on LB solid media  
226 without antibiotics at 37°C for 4 h, and 30°C for 20 h, then the mixture was spread on  
227 M9 solid plates and incubated at 30°C for 48 h with 50 mg/L gentamicin, after it was  
228 resuspended and washed using saline solution. Finally, the correct transconjugants  
229 were washed and plated on LB-sucrose agar medium for plasmid elimination (29).  
230 The gene engineered groups were obtained by inserting a *lacZ* promoter with the  
231 genes *FdFNR* before *cyp168A1* (PLAC-HS9), or inserting a single *lacZ* promoter with  
232 the genes *FdFNR* followed *cyp168A1* (HS9-DW), or combined the operations of  
233 PLAC-HS9 and HS9-DW to get PLAC-DW. The *lacZ* promoter sequence was

234 amplified from clone vector pMD18T.

235 The expression vector pUC18k was used for gene complement in *P. aeruginosa*.

236 The new expression plasmid pUC18k-*cyp168A1* was electrotransferred to strain HS9.

237 Electrocompetent cells were prepared as follows: first, the strain was cultured in LB

238 medium at 30°C after OD600 reached 0.6, and then the cells were pelleted at 4,000

239 rpm for 10 min, after incubating on ice for 20 min; finally, the cell pellets were

240 washed twice using electroporation buffer (10% glycerol) (30). Correct transformants

241 were verified by PCR and the cells were further incubated in LB medium with

242 corresponding antibiotics.

243

## 244 **Results**

245 **Genomic and proteomic profiles of strain HS9.** Whole genome sequencing was

246 performed, and the sequence was assembled into a single circular chromosome

247 without gaps (Fig. S1A). The circular chromosome is 6,876,988 bp in size, with a G +

248 C content of 66.2% and 6,421 coding sequences (CDSs). Further analysis indicated

249 that there were 157 CDSs annotated as related to metabolism of aromatic compounds

250 (Fig. S1B). To explore functional genes involved in HBCD degradation, a proteomic

251 analysis was carried out to compare the expression of proteins from cells incubated in

252 the presence or absence of 1 mg/L HBCDs MSM media. A total of 1,770 proteins

253 were identified, accounting for 27.6% of the genomic putative CDSs in strain HS9.

254 Normalization was performed to average the abundance of all peptides. Differentially

255 expressed proteins were filtered if their fold changes were over 2.0-fold with

256 significance > 20 (PEAKS Significance B Algorithm, p-value < 0.01) and if they had  
257 two unique peptides.

258 The expression of 277 proteins was significantly changed ( $\geq$  2-fold change,  
259  $P$ -value < 0.01), of which 190 proteins were up regulated and 87 were down-regulated  
260 (Fig. S1C). The up regulated proteins were divided into 25 categories by Clusters of  
261 Orthologous Groups (COGs) analysis (Fig. S1D). To narrow the search, the most  
262 significantly changed proteins ( $\geq$  10-fold change,  $P$ -value < 0.01) are summarized in  
263 Fig. S2, and the HBCD-induced proteins are listed in Table S1. No annotated  
264 dehalogenases were identified among the 277 up regulated proteins, while the  
265 expression of the NADH reductase (HS5738), heme d1 biosynthesis protein (NirF)  
266 (HS1898) and iron (III) dicitrate transport protein (FecA) (HS1283) were up regulated  
267 with fold changes of 5.81, 217.80, and  $+\infty$ , respectively. As many up regulated genes  
268 were related to electron donating, the functional genes that cooperated with electron  
269 donor were considered as possible HBCD degrading genes.

270 Many genes related to heavy metal were up regulated, including zinc and  
271 mercury transporting ATPase (EC 3.6.3.3), heavy metal sensor histidine kinase,  
272 copper resistance protein (CopC),  $\text{Na}^+$ /alanine symporter, iron (III) dicitrate transport  
273 protein (FecA), and zinc protease. Moreover, genes correlated with basic bioactivity,  
274 such as D-lactate dehydrogenase, L-lactate dehydrogenase (EC 1.1.2.3), L-lactate  
275 permease, and succinate dehydrogenase were significantly up regulated.

276

277 **Identification of HBCD degrading genes.** To identify the possible genes involved in

278 HBCD degradation in cooperation with Ferredoxin-NADP (+) reductase, three  
279 cytochrome P450 (CYP) proteins were selected as candidates. RT-qPCR assays were  
280 carried out to further detect the mRNA expression levels of the potential genes (Fig.  
281 1A). The cytochrome P450 coding gene *cyp168A1* was up regulated in response to  
282 HBCDs with a fold change of 9.1. The HBCD consumption curve of strain HS9 was  
283 determined in a resting cell reaction system. The wild type of strain HS9 (WT) could  
284 degrade 1 mg/L HBCDs within 8 h. In addition, we also deleted or complemented the  
285 gene *cyp168A1*, and HBCD consumption capability of the mutant strain *Δcyp168A1*  
286 was eliminated. When the *cyp168A1* gene was complemented in *Δcyp168A1*, the  
287 HBCD degradation capability of strain *Wcyp168A1* recovered to the same value as  
288 strain HS9 (Fig. 1B).

289

290 **Verification of electron donor capability of cell free system-FdFNR.** To confirm  
291 the donor supplying ability of FdFNR, potassium ferricyanide ( $K_3[Fe(CN)_6]$ ) was  
292 used as the receptor of the free donor. Compared to the control group, the absorbance  
293 of  $K_3[Fe(CN)_6]$  at A340 decreased to zero over 5 min, and the color feature (yellow)  
294 of  $K_3[Fe(CN)_6]$  disappeared (Fig. 2A). Results showed that the cell free system was  
295 able to oxidize NADH to  $NAD^+$  with an electron acceptor present.

296

297 **CYP168A1 is an efficient debromination enzyme.** The gene *cyp168A1* was  
298 amplified and expressed in pET28a in *E. coli* BL21(DE3). The heterologously  
299 expressed  $6 \times His$ -CYP168A1 was successfully purified, with a molecular mass of 50



300 kDa (Fig. 2B), and the western blot analysis demonstrated the purified protein (Fig.  
301 S3A). The CO-difference spectrum showed that the purified protein has a strong  
302 absorbance at 450 nm (Fig. 2C). Results of enzyme activity detection showed that  
303 CYP168A1 degraded HBCDs in the presence of NADH in the FdFNR system. The  
304 optimal temperature for CYP168A1 activity was at 30°C (Fig. S3B), The effect of  
305 temperature on CYP168A1 stability was monitored by circular dichroism  
306 spectroscopy (CDS) (JASCO, Japan), which showed that CYP168A1 began to  
307 degenerate at temperatures above 35°C (Fig. S3C). Kinetic analysis revealed that the  
308  $V_{max}$  and  $K_m$  were 0.73 U/mg and 0.35 mM (Fig. 2D), respectively. Most metal ions,  
309 including  $Ca^{2+}$ ,  $Co^{2+}$ ,  $Cu^{2+}$ ,  $MoO_4^{2+}$ , enhanced enzyme activity, while  $Zn^{2+}$  and  $K^+$  did  
310 not (Fig. S3D).

311

312 **Product analysis and  $^{18}O$  isotope experiments.** The products of the reaction  
313 catalyzed by CYP168A1 were identified using LC-TOF-MS, based on the mass  
314 spectra ( $m/z$ ) of the target products. Products with molecular weights at  $[M-H]^-$   
315 612.7000, 614.7000, and 616.7000, or 576.7240 and 578.7219 were detected. The  
316 results were matched to the previously reported standard compounds PBCDOHs and  
317 two tetrabromocyclododecadiols (TBCDDOH<sub>5</sub>) (Fig. 3AB). Products with molecular  
318 weights at  $[M-H]^-$  450.8949, 388.9792, 325.0679 and 263.1655 were also detected  
319 (Fig. 3C-F). The bromide was detected by ion chromatography analysis (Fig. S4).  
320 These products suggest that CYP168A1 can degrade HBCDs through a debromination  
321 and hydrogenation process, and one oxygen atom was added to the product in each

322 step of the reaction. To determine the source of the oxygen that participates in the  
323 reaction,  $^{18}\text{O}$  isotope experiments were carried out as mentioned above. Products in  
324  $^{18}\text{O}_2$  group had molecular weights of [M-H] $^-$  611.5232, 612.6262, and 613.5282,  
325 which match to PBCD $^{16}\text{OHs}$  (Fig. 4A). In the  $^{16}\text{O}$ -Not lyophilized and  
326  $^{16}\text{O}$ -Lyophilized groups, PBCD $^{16}\text{OHs}$  were detected (Fig. 4B, 4C). Thus,  
327 lyophilization would not inactivate the enzyme activity. In contrast, products  
328 containing  $^{18}\text{O}$ , with molecular weights of [M-H] $^-$  612.7000, 614.7000, 616.7000, and  
329 617.4908, were only detected in the  $\text{H}_2^{18}\text{O}$  group (Fig. 4D). Comparing the results of  
330 Fig. 4A, B, and C with Fig. 4D,  $^{18}\text{O}$  from  $\text{H}_2^{18}\text{O}$  was added to PBCDOHs, and no  $^{18}\text{O}$   
331 labeled products formed in the  $^{18}\text{O}_2$  group. The results confirmed that the oxygen in  
332 PBCD $^{18}\text{OHs}$  was derived from  $\text{H}_2^{18}\text{O}$ . All the corresponding TIC spectrums for  
333 products detection are shown in Fig. S5 and Fig. S6. The proposed pathway of HBCD  
334 degradation catalyzed by CYP168A1 is shown in Fig. 5.

335

336 **Enhancement of degrading capacity of strain HS9.** To enhance the degrading  
337 capacity of strain HS9, the expression of gene *cyp168A1* and the combined donor  
338 supplying system FdFNR were increased with a promoter *lacZ* was added as Fig. 6A.  
339 The gene engineering modes and comparison of the HBCDs degrading ability of the  
340 wild-type HS9 (WT), mutants PLAC-HS9, HS9-DW, and PLAC-DW are shown in  
341 Fig. 6B. The cell growth and degrading rates of the mutants were detected in the  
342 MSM-HBCDs system, and the results showed that the degrading rates of strain  
343 HS9-DW were improved, compared to WT. However, increase the gene *cyp168A1*

344 expression cannot improve the degrading rate of HBCDs.

345

346 **Phylogenetic analysis.** Several amino acid sequences of dehalogenases CYPs, such  
347 as CYP7A11, CYP81A3v2 (17), CYP1A1, CYP2C11, CYP26B1 (13), CYP2E1 (15),  
348 CYP3A4 (17), CYP101 (14) and P450BM-1 (10), were compared, and the results  
349 showed that CYP168A1 was most closely related to CYP101 (Fig. 7).

350

### 351 **Discussion**

352 Hexabromocyclododecanes (HBCDs) have become a global research focus, due to  
353 their widespread pollution and serious harm to human health, such as inducing cancer  
354 (31), disrupting liver and thyroid hormones (32-33), and causing reproductive  
355 disorders (34). Several bacteria have been discovered from natural environments that  
356 can degrade HBCDs, such as *Pseudomonas* sp. HB01, *Bacillus* sp. HBCD-sjtu,  
357 *Achromobacter* sp. HBCD-1, *Achromobacter* sp. HBCD-2, and *P. aeruginosa* strain  
358 HS9 (35-38). Corresponding pathways have been proposed for these strains, but the  
359 specific molecular mechanisms of the degradation have not been revealed. In this  
360 study, the functional enzymes for HBCDs degradation from *P. aeruginosa* strain HS9  
361 was characterized.

362 Proteomic analysis comparing the expression of proteins of the cells incubated  
363 was carried out with MSM medium in the presence or absence of 1 mg/L HBCDs, and  
364 the results showed that environmental stress response genes like lactate  
365 dehydrogenases (LDH) were up regulated in the HBCD group. *Enterococcus faecalis*

366 has general resistance to very different environmental stresses, depending on the  
367 ability to maintain redox balance via LDH (39). In addition, decreases and increases  
368 in salinity concentrations sharply increase the LDH activity of *Neanthes*  
369 *arenaceodentata* (40). Moreover, succinate dehydrogenase was up regulated, which  
370 could catalyze succinate to fumarate when a FADH was formed. Based on the above  
371 information, we propose that the resistance of strain HS9 to HBCD stress occurs due  
372 to maintaining the balance of reducing power in vivo, coupled with HBCD  
373 degradation. HBCD could induce the expression of *cyp168A1* of strain HS9, while the  
374 CYP168A1 cooperation with electron donators, and the electron transport and stress  
375 resistance reactions (related to lactate dehydrogenases or succinate dehydrogenase)  
376 were used to balance the electron supply in vivo.

377 In nature, cytochrome P450 (CYP) enzymes participate in degrading large  
378 amounts of environmental pollutants. Typically, CYP monooxygenases introduce a  
379 single oxygen atom into their substrates (41-43). However, there are few reports about  
380 CYP enzymes simultaneously catalyzing debromination and hydrogenation reactions  
381 (44). In this study, a novel CYP (CYP168A1) was shown to be the initial  
382 dehalogenase enzyme in HBCD biodegradation. The gene *cyp168A1* was cloned and  
383 expressed in *E. coli* and the enzymatic properties of the purified CYP168A1 were  
384 investigated. The *K<sub>m</sub>* of CYP168A1 for HBCDs was 0.35 mM, while the *K<sub>m</sub>* of  
385  $\gamma$ -HBCD for LinB was  $1.82 \pm 0.60 \mu\text{M}$ , the affinity for HBCD to LinB is almost 1,000  
386 times than that to CYP168A1. However, biochemistry information for the other two  
387 major HBCD isomers to LinB was still limited. The affinity of CYP168A1 to HBCDs

388 was lower than that of LinA/B, it matched the lower degrading rate of strain HS9,  
389 compared to other HBCD degraders.

390 Considering the toxicity of HBCDs to the environment and humans, comparative  
391 metabolism studies and *in vitro* activity tests indicated that the human liver CYP3A4,  
392 maize CYPs, and male rat CYPs can degrade different HBCD isomers. To trace the  
393 source of gene *cyp168A1*, phylogenetic analysis was carried out. Several mono- and  
394 dihydroxylated metabolites of HBCDs are formed through catalyzing with the human  
395 liver CYP3A4, maize CYPs, and male rat CYPs, with mono-OH-HBCDs detected as  
396 the major metabolites (6, 17, 43). However, the products of HBCDs catalyzed by  
397 CYP168A1 were PBCDOHs and TBCDDOHs, generated from the debromination and  
398 hydrogenation processes of HBCDs, of which PBCDOHs were also identical to that  
399 produced by strain HS9 in HBCDs-MSM medium (21). This result revealed the  
400 difference of HBCDs biodegradation between eukaryotic cells and prokaryotic  
401 microorganisms.

402 In the reactions of 1,2-halododecanoic acids oxidation catalyzed by both CYP4A  
403 (44) and CYP52A (45), oxygen in 1,2-Hydroxydodecanoic acids derives from water,  
404 not from molecular oxygen, which was introduced by hydrolysis of an initially formed  
405 oxohalonium ( $R-X^+-O^-$ ) metabolite. The results of  $^{18}O$  isotope labeling reactions  
406 showed that  $H_2O$  serves as the source of the oxygen atom incorporated into  
407 PBCDOHs (Fig. 4). Mechanism of the oxygen addition was the same as oxidation of  
408 1,2-halododecanoic acids by CYP4A and CYP52A. The present study revealed a  
409 novel mechanism of CYP to catalyze the brominated organic compounds.

410 In summary, this study reveals a new catalytic mechanism of CYP168A1 for the  
411 degradation of HBCDs, in which the debromination and hydrogenation reactions are  
412 carried out one after another. The <sup>18</sup>O isotope experiments show that the oxygen  
413 added into hydrated products were from H<sub>2</sub>O. Engineering mutants of strain HS9 not  
414 only supplies new insights into biochemical properties of protein CYP168A1, but also  
415 serves as a model for enhancing the abilities of this strain in bioremediation.

416

#### 417 **Competing interests**

418 All the authors declare no competing interests.

419

#### 420 **Authors' contributions**

421 LH and HT outset and designed experiments. LH and WW performed experiments.

422 HT and PX contributed reagents and materials. LH, HT, ZG, and PX wrote the paper.

423 All Authors discussed and revised the manuscript. All Authors commented on the

424 manuscript before submission. All authors read and approved the final manuscript.

425

#### 426 **Acknowledgements**

427 This study was supported by the grants from National Key Research and

428 Development Project (2018YFA0901200), from Shanghai Excellent Academic

429 Leaders Program (20XD1421900), from 'Shuguang Program' (17SG09) supported by

430 Shanghai Education Development Foundation and Shanghai Municipal Education

431 Commission, from the National Natural Science Foundation of China (31770114),

432 and from the Science and Technology Commission of Shanghai Municipality

433 (17JC1403300).

434 **References**

- 435 1. Fonseca VM, Jr VJF, Araujo AS, Carvalho LH, Souza AG. 2005. Effect of  
436 halogenated flame-retardant additives in the pyrolysis and thermal degradation of  
437 polyester sisal composites. *J Therm Anal Calorim* 79:429–433.  
438 <https://link.springer.com/article/10.1007/s10973-005-0079-x>
- 439 2. Tang H, Wang L, Wang W, Yu H, Zhang K, Yao Y, Xu P. 2013. Systematic  
440 unraveling of the unsolved pathway of nicotine degradation in *Pseudomonas*.  
441 *PLoS Genetics* 9: e1003923. <https://www.ncbi.nlm.nih.gov/pubmed/24204321>
- 442 3. Heeb NV, Wyss SA, Geueke B, Fleischmann T, Kohler HPE, Lienemann P. 2014.  
443 LinA2, a HCH-converting bacterial enzyme that dehydrohalogenates HBCDs.  
444 *Chemosphere* 107:194–202. DOI: [10.1016/j.chemosphere.2013.12.035](https://doi.org/10.1016/j.chemosphere.2013.12.035)
- 445 4. Heeb NV, Zindel D, Geueke B, Kohler HPE, Lienemann P. 2012.  
446 Biotransformation of hexabromocyclododecanes (HBCDs) with linB—an  
447 HCH-converting bacterial enzyme. *Environ Sci Technol* 46:6566–6574. DOI:  
448 [10.1021/es2046487](https://doi.org/10.1021/es2046487)
- 449 5. Heeb NV, Manuel M, Simon W, Birgit G, Hans-Peter EK, Peter L. 2018. Kinetics  
450 and stereochemistry of LinB-catalyzed  $\delta$ -HBCD transformation: Comparison of in  
451 vitro and in silico results. *Chemosphere* 207:118–129. DOI:  
452 [10.1016/j.chemosphere.2018.05.057](https://doi.org/10.1016/j.chemosphere.2018.05.057)
- 453 6. Dimaano NG, Yamaguchi T, Fukunishi K, Tominaga T, Iwakami S. 2020.  
454 Functional characterization of cytochrome P450 CYP81A subfamily to disclose  
455 the pattern of cross-resistance in *Echinochloa phyllopogon*. *Plant Mol Biol*



- 456 102:403–416. DOI: [10.1007/s11103-019-00954-3](https://doi.org/10.1007/s11103-019-00954-3)
- 457 7. Ding J, Guotao LG, Huang Z. 2018. Research progress in microbial cytochrome  
458 P450 and xenobiotic metabolism. *Chinese J Appl Environ Biol* 3:657–662.
- 459 8. Karl F, Roger B. 2000. Cytochrome P4501A induction potencies of polycyclic  
460 aromatic hydrocarbons in a fish hepatoma cell line: Demonstration of additive  
461 interactions. *Environ Toxicol Chem* 19:2047–2058.  
462 <https://setac.onlinelibrary.wiley.com/doi/10.1002/etc.5620190813>
- 463 9. Brack W, Schirmer K, Kind T, Schrader S, Schüürmann G. 2010. Effect-directed  
464 fractionation and identification of cytochrome P4501 A-inducing halogenated  
465 aromatic hydrocarbons in a contaminated sediment. *Environ Toxicol Chem*  
466 21:2654–2662.  
467 <https://setac.onlinelibrary.wiley.com/doi/full/10.1002/etc.5620211218>
- 468 10. Sakaki T, Yamamoto K, Ikushiro S. 2013. Possibility of application of cytochrome  
469 P450 to bioremediation of dioxins. *Biotechnol Appl Biochem* 60:65–70.  
470 <https://www.ncbi.nlm.nih.gov/pubmed/23586993>
- 471 11. Guo F, Iwakami S, Yamaguchi T, Uchino A, Sunohara Y, Matsumoto H. 2019.  
472 Role of CYP81A cytochrome P450s in clomazone metabolism in *Echinochloa*  
473 *phyllopogon*. *Plant Sci* 283:321–328. DOI: [10.1016/j.plantsci.2019.02.010](https://doi.org/10.1016/j.plantsci.2019.02.010)
- 474 12. Iwakami S, Kamidate Y, Yamaguchi T, Ishizaka M, Endo M, Suda H, Nagai K,  
475 Sunohara Y, Toki S, Uchino A, Tominaga T, Matsumoto H. 2018. CYP81A P450s  
476 are involved in concomitant cross-resistance to ALS and ACCase herbicides in  
477 *Echinochloa phyllopogon*. *New Phytol* 221:2112–2122.

- 478 <https://nph.onlinelibrary.wiley.com/doi/full/10.1111/nph.15552>
- 479 13. Sakaki T, Shinkyō R, Takita T, Ohta M, Inouye K. 2002. Biodegradation of  
480 polychlorinated dibenzo-p-dioxins by recombinant yeast expressing rat CYP1A  
481 subfamily. *Arch Biochem Biophys* 401:0–98.  
482 <https://www.ncbi.nlm.nih.gov/pubmed/12054491>
- 483 14. Yan D, Liu H, Zhou NY. 2006. Conversion of *Sphingobium chlorophenolicum*  
484 ATCC 39723 to a hexachlorobenzene degrader by metabolic engineering. *Appl*  
485 *Environ Microbiol* 21:18. DOI: [10.1128/AEM.72.3.2283-2286.2006](https://doi.org/10.1128/AEM.72.3.2283-2286.2006)
- 486 15. Singh S, Sherkhane PD, Kale SP, Eapen S. 2011. Expression of a human  
487 cytochrome P450 2E1 in *Nicotiana tabacum* enhances tolerance and remediation  
488 of  $\gamma$ -hexachlorocyclohexane. *N Biotechnol* 28:423–429. DOI:  
489 [10.1016/j.nbt.2011.03.010](https://doi.org/10.1016/j.nbt.2011.03.010)
- 490 16. Huang H, Wang D, Wen B, Lv J, Zhang S. 2019. Roles of maize cytochrome P450  
491 (CYP) enzymes in stereo-selective metabolism of hexabromocyclododecanes  
492 (HBCDs) as evidenced by in vitro degradation, biological response and in silico  
493 studies. *Sci Total Environ* 656:364–372. DOI: [10.1016/j.scitotenv.2018.11.351](https://doi.org/10.1016/j.scitotenv.2018.11.351)
- 494 17. Erratico C, Zheng X, Nele VDE, Tomy GT, Covaci A. 2016. Stereo-selective  
495 metabolism of  $\alpha$ -,  $\beta$ - and  $\gamma$ -hexabromocyclododecanes (HBCDs) by human liver  
496 microsomes and CYP3A4. *Environ Sci Technol* 50:8263–8273.  
497 <https://www.sciencedirect.com/science/article/pii/S1385894719312549>
- 498 18. Esslinger S, Becker R, Maul R, Nehls I. 2011. Hexabromocyclododecane  
499 enantiomers: microsomal degradation and patterns of hydroxylated metabolites.

- 500 *Environ Sci Technol* 45:3938–3944. <https://pubs.acs.org/doi/10.1021/es1039584>
- 501 19. Zheng X, Erratico C, Abdallah MA, Negreira N, Luo X, Mai B, Covaci A. 2015.
- 502 In vitro metabolism of BDE-47, BDE-99, and  $\alpha$ -,  $\beta$ -,  $\gamma$ -HBCD isomers by chicken
- 503 liver microsomes. *Environ Res* 143:221–228.
- 504 <https://www.sciencedirect.com/science/article/pii/S0013935115301201>
- 505 20. Zheng X, Erratico C, Luo X, Mai B, Covaci A. 2016. Oxidative metabolism of
- 506 BDE-47, BDE-99, and HBCDs by cat liver microsomes: implications of cats as
- 507 sentinel species to monitor human exposure to environmental pollutants.
- 508 *Chemosphere* 151:30–36. DOI: 10.1016/j.chemosphere.2016.02.054
- 509 21. Huang L, Wang W, Shah SB, Hu H, Xu P, Tang H. 2019. The HBCDs
- 510 biodegradation using a *Pseudomonas* strain and its application in soil
- 511 phytoremediation. *J Hazard Mater* 380:e120833.
- 512 <https://www.sciencedirect.com/science/article/pii/S0304389419307861>
- 513 22. Tang H, Yao Y, Zhang D, Meng X, Wang L, Yu H, Ma L, Xu P. 2011. A novel
- 514 NADH-dependent and FAD-containing hydroxylase is crucial for nicotine
- 515 degradation by *Pseudomonas putida*. *J Biol Chem* 286:39179–39187.
- 516 <https://www.ncbi.nlm.nih.gov/pmc/articles/PMC3234743>
- 517 23. Lu X, Wang W, Zhang L, Hu H, Xu P, Wei T, Tang H. 2019. Molecular
- 518 mechanism of *N, N*-Dimethylformamide degradation in a *Methylobacterium* sp.
- 519 strain DM1. *Appl Environ Microbiol* 85:e00275–319.
- 520 <https://aem.asm.org/content/85/12/e00275-19>
- 521 24. Yao X, Tao F, Zhang K, Tang H, Xu P. 2017. Multiple roles of two efflux pumps

- 522 in a polycyclic aromatic hydrocarbon-degrading, *Pseudomonas putida* strain B6-2  
523 (DSM 28064). *Appl Environ Microbiol* 83:e01882-1917. DOI:  
524 [10.1128/AEM.01882-17](https://doi.org/10.1128/AEM.01882-17)
- 525 25. Yu H, Tang H, Zhu X, Li Y, Xu P. 2015. Molecular mechanism of nicotine  
526 degradation by a newly isolated strain, *Ochrobactrum* sp. strain SJY1. *Appl*  
527 *Environ Microbiol* 81:272–281. <https://aem.asm.org/content/aem/81/1/272.full.pdf>
- 528 26. Yu J, Zhang Y, Wang Z. 2018. Chicken (*Gallus gallus*) HNF1 $\alpha$  expression in  
529 *Escherichia coli* and its purification. *J Agricul Biotechnol* 3:e1.
- 530 27. Funhoff E G, Bauer U, Garcia-Rubio I, Beilen V J B. 2006. CYP153A6, a soluble  
531 p450 oxygenase catalyzing terminal-alkane hydroxylation. *J Biol Chem* 188:  
532 5220–5227. <https://jbc.asm.org/content/188/14/5220>
- 533 28. Yu H, Hausinger RP, Tang H, Xu P. 2014. Mechanism of the  
534 6-Hydroxy-3-succinoyl-pyridine 3-monooxygenase flavoprotein from  
535 *Pseudomonas putida* S16. *J Biol Chem* 289:29158–29170. DOI:  
536 [10.1074/jbc.M114.558049](https://doi.org/10.1074/jbc.M114.558049)
- 537 29. Qu Y, Ma Q, Liu Z, Wang W, Tang H, Zhou J, Xu P. 2017. Unveiling the  
538 biotransformation mechanism of indole in a *Cupriavidus* sp. strain. *Mol Microbiol*  
539 106:905–918. <https://onlinelibrary.wiley.com/doi/full/10.1111/mmi.13852>
- 540 30. Jiang Yi, Tang H, Wu G, Xu P. 2015. Functional identification of a novel gene,  
541 *moaE*, for 3-Succinoylpyridine degradation in *Pseudomonas putida* S16. *Sci Rep*  
542 5:13464. DOI: [10.1038/srep13464](https://doi.org/10.1038/srep13464)
- 543 31. Yvonne F, Inga B. 2009. Technical pentabromodipheny ether and

- 544 hexabromocyclododecane as activators of the pregnane-X-receptor (PXR).  
545 *Toxicol.* 29:656–661. DOI: [10.1016/j.tox.2009.07.009](https://doi.org/10.1016/j.tox.2009.07.009)
- 546 32. Palace VP, Pleskach K, Halldorson T, Danell R, Wautier K, Evans B. 2008.  
547 Biotransformation enzymes and thyroid axis disruption in juvenile rainbow trout  
548 (*Oncorhynchus mykiss*) exposed to hexabromocyclododecane diastereoisomers.  
549 *Environ Sci Technol* 42:1967–1972. DOI: [10.1021/es702565h](https://doi.org/10.1021/es702565h)
- 550 33. Ven LTMVD, Verhoef A, Kuil TVD, Slob W, Leonards PEG, Visser TJ, Hamers T,  
551 Herlin M, Hakansson H, Olausson H, Piersma A, Vos J. 2006. A 28-day oral dose  
552 toxicity study enhanced to detect endocrine effects of hexabromocyclododecane in  
553 Wistar rats. *Toxicol Sci* 94:281–292.  
554 <https://www.ncbi.nlm.nih.gov/pubmed/16984958>
- 555 34. Makoto E, Sakiko F, Mutsuko H K, Mariko M. 2008. Two-generation  
556 reproductive toxicity study of the flame retardant hexabromocyclododecane in rats.  
557 *Reprod Toxicol* 25:335–351.  
558 <https://www.sciencedirect.com/science/article/abs/pii/S0890623807003383>
- 559 35. Gao Y, Zhang X, Yang C. 2011. Photodegradation of hexabromocyclododecane in  
560 water. *Environ Chem* 30:598–603.
- 561 36. Zhao YY, Zhang XH, Sojinu OS. 2010. Thermodynamics and photochemical  
562 properties of alpha, beta, and gamma- hexabromocyclododecanes: a theoretical  
563 study. *Chemosphere* 80:150–156. DOI: [10.1016/j.chemosphere.2010.04.002](https://doi.org/10.1016/j.chemosphere.2010.04.002)
- 564 37. Zhou D, Wu Y, Feng X, Chen Y, Wang Z, Tao T, Wei D. 2014. Photodegradation  
565 of hexabromocyclododecane (HBCD) by Fe(III) complexes/H<sub>2</sub>O<sub>2</sub> under simulated

- 566 sunlight. *Environ Sci Pollut Res* 21:6228–6233. DOI: [10.1007/s11356-014-2553-0](https://doi.org/10.1007/s11356-014-2553-0)
- 567 38. Nyholm J., Lundberg C, Andersson PL. 2010. Biodegradation kinetics of selected  
568 brominated flame retardants in aerobic and anaerobic soil. *Environ Pollut*  
569 158:2235–2240.  
570 <https://www.sciencedirect.com/science/article/pii/S0269749110000710>
- 571 39. Rana NF, Sauvageot N, Laplace JM, Bao Y, Nes I, Rince A, Posteraro B,  
572 Sanguinetti M, Hartke A. 2013. Redox balance via lactate dehydrogenase is  
573 important for multiple stress resistance and virulence in *Enterococcus faecalis*.  
574 *Infect Immun* 81:2662–2668. <https://iaa.asm.org/content/81/8/2662>
- 575 40. Cripps RA, Reish DJ. 1973. The effect of environmental stress on the activity of  
576 malate dehydrogenase and lactate dehydrogenase and lactate dehydrogenase in  
577 *Neanthes arenacedentata* (Annelida: Polychaeta). *Comp Biochem Phys B*  
578 46:123–133. DOI: [10.1016/0305-0491\(73\)90052-7](https://doi.org/10.1016/0305-0491(73)90052-7)
- 579 41. Durairaj P, Hur JS, Yun H. 2016. Versatile biocatalysis of fungal cytochrome  
580 P450 monooxygenases. *Microb Cell Fact* 15:125.  
581 <https://www.ncbi.nlm.nih.gov/pmc/articles/PMC4950769>
- 582 42. Urlacher VB, Girhard M. 2019. Cytochrome P450 monooxygenases in  
583 biotechnology and synthetic biology. *Trends Biotechnol* 37:882–897.  
584 <https://www.sciencedirect.com/science/article/pii/S0167779919300010>
- 585 43. Hakk H. 2016. Comparative metabolism studies of hexabromocyclododecane  
586 (HBCD) diastereomers in male rats following a single oral dose. *Environ Sci*  
587 *Technol* 50:89–96. <https://pubs.acs.org/doi/10.1021/acs.est.5b04510>

- 588 44. He X, Cryle MJ, De VJJ, Ortiz dMPR. 2005. Calibration of the channel that  
589 determines the  $\omega$ -hydroxylation regiospecificity of cytochrome P4504A1. *J Biol*  
590 *Chem* 280: 22697–22705. DOI: [10.1074/jbc.M502632200](https://doi.org/10.1074/jbc.M502632200)
- 591 45. Kim D, Cryle MJ, De VJJ, Ortiz dMPR. 2007. Functional expression and  
592 characterization of cytochrome P450 52A21 from *Candida albicans*. *Arch*  
593 *Biochem Biophys* 464: 213–220.

**Table 1. The primers used in this study.** (The underline represents homologous sequences to the constructed vector)

| Names      | Sequence (3' - 5')                                 | Function                                |
|------------|----------------------------------------------------|-----------------------------------------|
| GmF        | <u>CCCAAGCTT</u> ATGTTACGCAGCAGCAACGA              | Replacement of resistance gene          |
| GmR        | CTAGCTAGCTTAGGTGGCGTACTTGGGT                       | Replacement of resistance gene          |
| Fcyp168A1  | CCGGAATTCATGGACGACGCATTCAGCGA                      | Construction of pET28a- <i>cyp168A1</i> |
| Rcyp168A1  | <u>CCCAAGCTT</u> CTCGCAGGTCTTCTGAGCGT              | Construction of pET28a- <i>cyp168A1</i> |
| AFcyp168A1 | <u>TATGACATGATTACGAATTC</u> ATGGACGACGCATTCAGCGA   | Gene knockout                           |
| ARcyp168A1 | <u>GTTATAAATTTGGAGTGTG</u> ACACGGCGTCGGGGCCGAAG    | Gene knockout                           |
| BFcyp168A1 | <u>TCACACTCCAAATTTATAAC</u> GCGGGCGAACGCGGTGGAGGA  | Gene knockout                           |
| BRcyp168A1 | <u>AGGTCGACTCTAGAGGATCC</u> CTCGCAGGTCTTCTGAGCGT   | Gene knockout                           |
| Uplac-A1F  | <u>TGACATGATTACGAATTC</u> CGAATACCAGAACCAGGGCA     | Construction of PLAC-HS9/PLAC-DW        |
| Uplac-A1R  | <u>TGAGTGAGCTAACTCACATT</u> GGCCCTTGCTCCGCTGGGT    | Construction of PLAC-HS9/PLAC-DW        |
| UplacF     | AATGTGAGTTAGCTCACTCA                               | Construction of PLAC-HS9/PLAC-DW        |
| UplacR     | <u>TCGCTGAATGCGTCGTCC</u> ATGGCGTAATCATGGTCATAGC   | Construction of PLAC-HS9/PLAC-DW        |
| Uplac-B1F  | ATGGACGACGCATTCAGCGA                               | Construction of PLAC-HS9/PLAC-DW        |
| Uplac-B1R  | <u>GCAGGTCGACTCTAGAGGATCC</u> CCCGGCATCGCCGTGGCTGG | Construction of PLAC-HS9/PLAC-DW        |
| Dplac-A2F  | <u>TGACATGATTACGAATTC</u> CCAGCCACGGCGATGCCGGG     | Construction of HS9-DW/PLAC-DW          |
| Dplac-A2R  | <u>TGAGTGAGCTAACTCACATT</u> CTACTCGCAGGTCTTCTGAG   | Construction of HS9-DW/PLAC-DW          |
| Dplac-F    | AATGTGAGTTAGCTCACTCA                               | Construction of HS9-DW/PLAC-DW          |
| Dplac-R    | <u>TCCAGCACGACGAAGGTC</u> ATGGCGTAATCATGGTCATAGC   | Construction of HS9-DW/PLAC-DW          |
| DFERF      | ATGACCTTCGTGCTGCTGGA                               | Construction of HS9-DW/PLAC-DW          |
| DFERR      | <u>GGCAGCCGGCTGATCCTG</u> CGTCACTTCTCGACGAAGGCGC   | Construction of HS9-DW/PLAC-DW          |
| Dplac-B2F  | CGCAGGATCAGCCGGCTGCC                               | Construction of HS9-DW/PLAC-DW          |
| Dplac-B2R  | <u>GCAGGTCGACTCTAGAGGATCC</u> GAGGCCGACGACTTCATGGA | Construction of HS9-DW/PLAC-DW          |
| cyp168A1cF | <u>GGTCGACTCTAGAGGATCC</u> CATGGACGACGCATTCAGCGA   | Gene complementation                    |



cyp168A1cR

AGGTCGACTCTAGAGGATCCCTCGCAGGTCTTCTGAGCGT

Gene complementation

---

595 **Figure legends**

596 **Fig. 1. Identification of functional proteins.** (A) RT-qPCR verification of the  
597 proposed functional genes in degrading HBCDs. In RT-qPCR assays, the treatment  
598 group used HBCDs as the sole carbon source and the control group used sodium  
599 citrate. HS651: putative cytochrome P450 hydroxylase; HS1037: cytochrome P450;  
600 HS6073 (*cyp168A1*): putative cytochrome P450 hydroxylase (B) Comparison of the  
601 HBCD degrading ability of the wild type HS9 (WT), *cyp168A1* deleted mutant strain  
602 (*Mcyp168A1*) and *cyp168A1* complemented strain (*Wcyp168A1*).

603

604 **Fig. 2. Characterization of CYP168A1.** (A) Verification of the electron donor  
605 capability of the cell free system-FdFNR. The protein expression of FdFNR was  
606 measured and shown by SDS-PAGE, the color feature (yellow) of  $K_3[Fe(CN)_6]$  was  
607 captured, and the full wavelength scanning shows the concentration of  $K_3[Fe(CN)_6]$  in  
608 the cell free system. (B) SDS-PAGE analysis of CYP168A1. M: protein marker; lane  
609 1, supernatant of the sonicated Bl21-pET28a-*cyp168A1*; lane 2, column effluent; lane  
610 3, 10 mM imidazole buffer washed effluent; lane 4, 45 mM imidazole washed effluent;  
611 lane 5, 70 mM imidazole washed effluent; lane 6, 100 mM imidazole washed effluent;  
612 lane 7, 150 mM imidazole washed effluent. (C) The CO-difference spectrum of  
613 CYP168A1. (D) Kinetic analysis of CYP168A1 (fitted to the Michaelis-Menten  
614 kinetics).

615

616 **Fig. 3. Identification of intermediates of HBCD degradation by LC-TOF-MS.** (A)  
617 Mass spectra of PBCDOHs. (B) Mass spectra of TBCDDOHs. (C)-(F) Corresponding

618 mass spectra of molecular weights ( $m/z$  450.8949) ( $m/z$  388.9792) ( $m/z$  325.0679) and  
619 ( $m/z$  263.1655).

620

621 **Fig. 4.  $^{18}\text{O}$  labeled products of HBCD degradation.** (A) Mass spectra extracted  
622 from the  $^{18}\text{O}$  group (PBCD $^{16}\text{OHs}$ ). (B) Mass spectra extracted from the  $^{16}\text{O}$ -Not  
623 lyophilized group (PBCD $^{16}\text{OHs}$ ). (C) Mass spectra extracted from the  
624  $^{16}\text{O}$ -Lyophilized group (PBCD $^{16}\text{OHs}$ ). (D) Mass spectra extracted from the  
625  $^{18}\text{O}$ -Lyophilized group (PBCD $^{18}\text{OHs}$ ).

626

627 **Fig. 5. Proposed pathway for HBCD degradation.** HBCDs were dehalogenated by  
628 CYP168A1, with a serial of hydroxy added. The undetected oxohalonium metabolites  
629 have been drawn in frame.

630

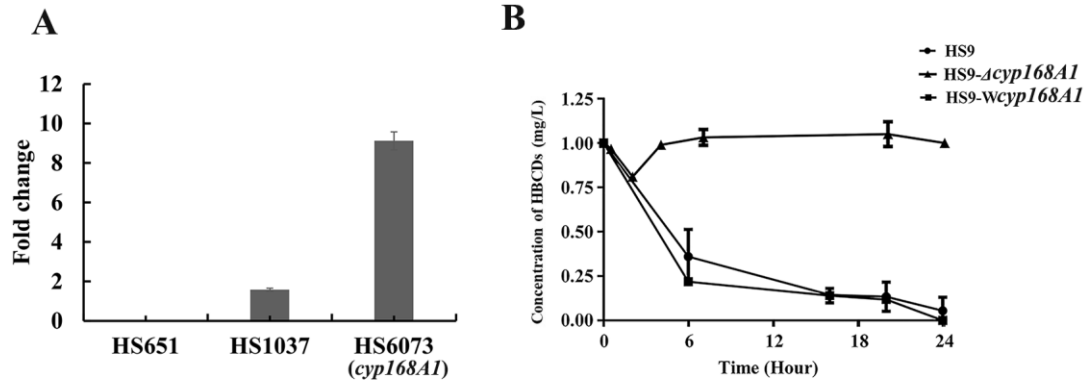
631 **Fig. 6.** Schematic for the gene engineering (A), and comparison of the HBCDs  
632 degrading ability of the wild-type HS9 (WT) and genome edited mutants PLAC-HS9,  
633 HS9-DW, and PLAC-DW (B).

634

635 **Fig. 7.** Phylogenetic tree analysis of CYP168A1 with reported cytochrome P450  
636 enzymes that function in dehalogenation.

637 Fig. 1

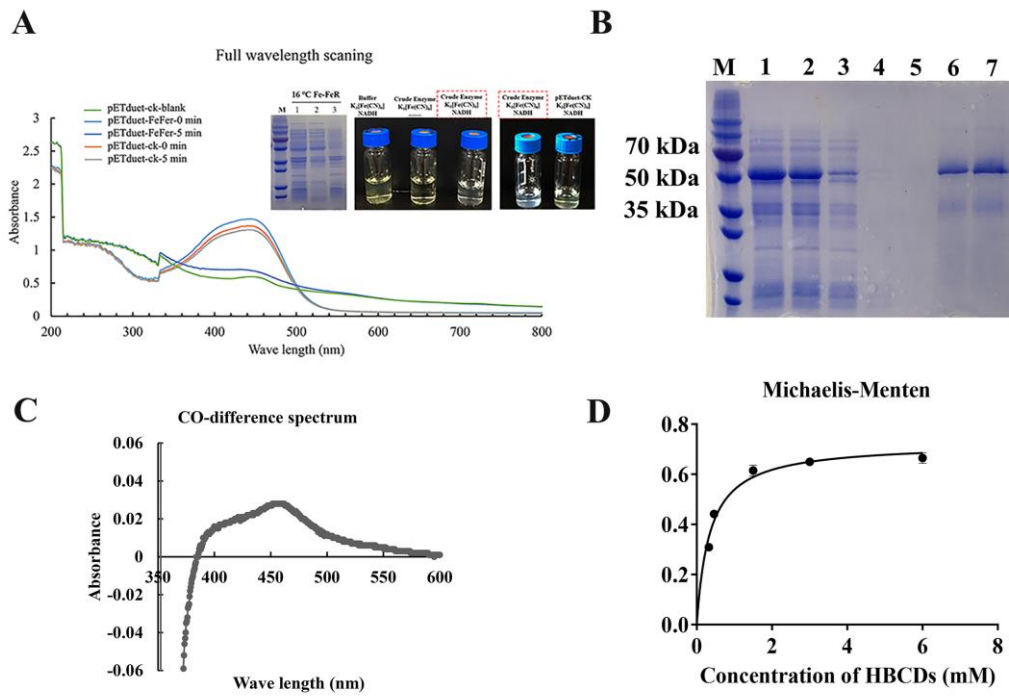
638



639

640 **Fig. 2**

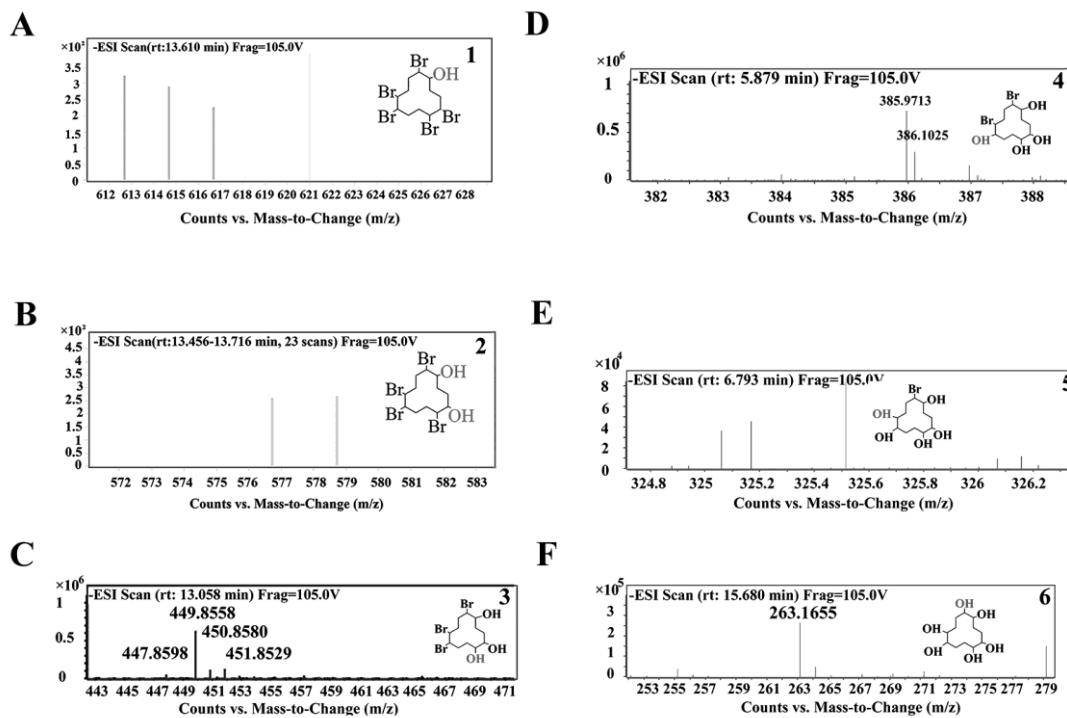
641



642

643 Fig. 3

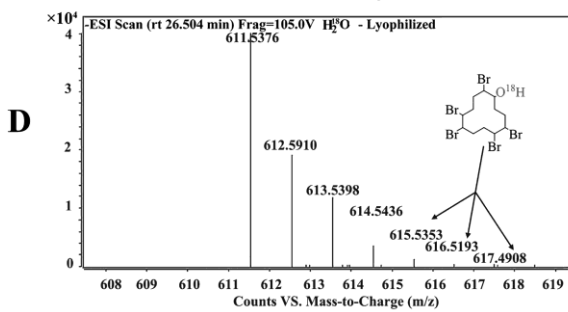
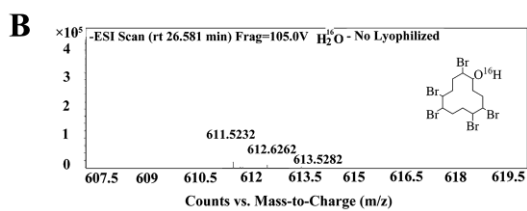
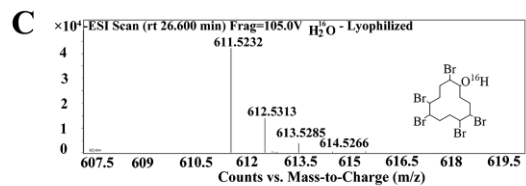
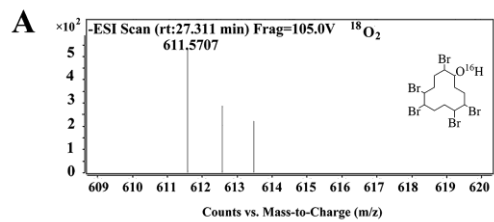
644



645

646 Fig. 4

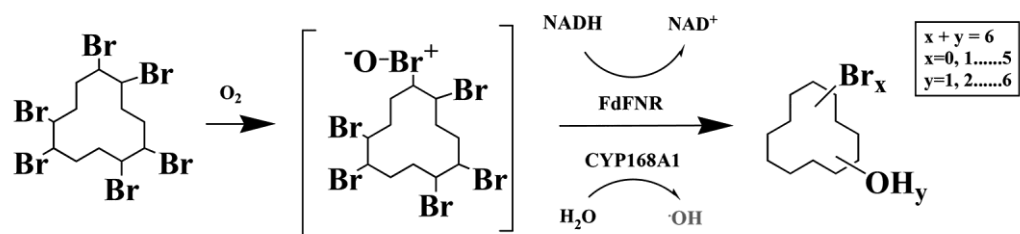
647



648

649 Fig. 5

650



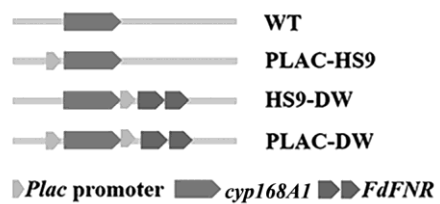
651



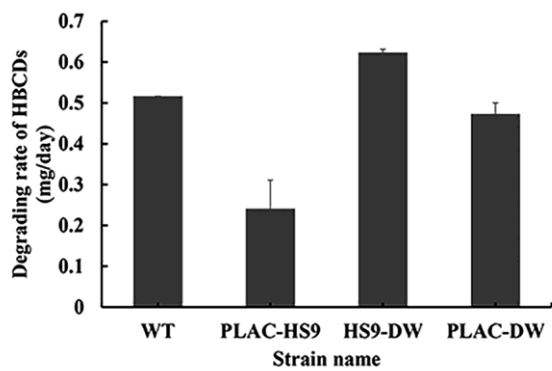
652 Fig. 6

653

**A**



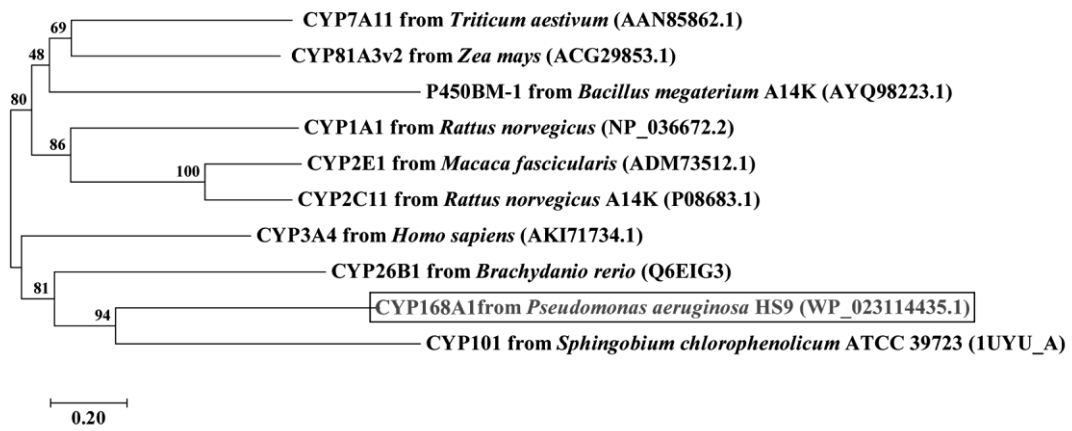
**B**



654

655 **Fig. 7**

656



657